Wiring efficiency of a metallizable DNA linker for site-addressable nanobioelectronic assembly

2007 Nanotechnology 18 424025

(http://iopscience.iop.org/0957-4484/18/42/424025)

IOP PUBLISHING NANOTECHNOLOGY
Nanotechnology **18** (2007) 424025 (9pp) doi:10.1088/0957-4484/18/42/424025

Wiring efficiency of a metallizable DNA linker for site-addressable nanobioelectronic assembly

Gary D Withey, Jin Ho Kim and Jimmy Xu

Division of Engineering, Brown University, 182 Hope Street, Providence, RI 02912, USA

Received 14 March 2007, in final form 26 April 2007
Published 21 September 2007
Online at stacks.iop.org/Nano/18/424025

Abstract
We report the first demonstration of DNA oligonucleotide tags used to address the site-specific assembly of multiple redox enzymes onto spatially distinct regions of a nanoelectronic platform, establishing a direct electrical contact. The resulting system constitutes a multiplexed carbon nanotube–redox protein biosensor capable of detecting varying concentrations of several different substances in real time. The efficiency and robustness of the enzyme linking scheme is explored in detail, showing a high degree of preservation of enzymatic activity and an efficient electrical contact at the enzyme–nanoelectrode interface. While five proteins have been used as a demonstration in this study, there is virtually no limit to the number of enzymes that could be bound in parallel using this linking strategy, which is universally applicable to all proteins due to the simple conjugation chemistry involved. We further demonstrate metallization of the linker in the presence of a divalent metal cation, inducing elevated electron transfer efficiency relative to the native DNA link.

(Some figures in this article are in colour only in the electronic version)

1. Introduction

Redox enzymes, due to their extraordinary inherent specificity and efficiency, have long been a subject of considerable interest to scientists working in bioelectronics. They constitute the functional elements that give rise to a great number of promising devices, of which perhaps the most prevalent are biosensors and biofuel cells [1–12]. Amperometric biosensing involves the immobilization of redox-active proteins at an electrode surface to establish an electrical contact to the enzyme's redox centre. The application of a specific redox potential and the cycling of a substrate-specific redox reaction at the electrode surface gives rise to electrocatalytic currents that indicate the presence and concentration of the substrate of interest. In recent years, novel nanomaterials such as carbon nanotubes (CNTs) and gold nanoparticles (AuNPs) have been demonstrated to promote direct electron transfer at the enzyme–electrode interface [4–12]. The size compatibility between proteins and these nano-featured electrodes allows closer access to the redox site than in the case of conventional flat electrodes [4]. Several factors influence the performance of bioelectronic devices. Of these, perhaps the most significant are preservation of active protein conformation and favourable orientation of the redox site towards the electrode surface [3, 5, 6, 13].

A wide variety of protein immobilization techniques have been explored, including physical adsorption, covalent attachment via cross-linking agents and assembly onto self-assembled monolayers (SAMs) [4–11]. Physical adsorption, the simplest of these methods, inherently results in a randomly oriented protein layer and also suffers from multiple points of contact between the enzyme and electrode surface that tend to cause denaturation of the protein and loss of enzymatic activity [3, 5]. This denaturing effect can be mitigated by cross-linkers and SAMs. The trade-off in this case is that the enzyme is placed at a greater distance, on average, from the electrode surface. These issues of orientation, denaturation and proximity are central to the design of bioelectronic devices, and will be discussed in greater detail in the following sections. Recently, nano-bioelectronic designs have begun to scale from singularly functional systems that sense a single substance to multiplexed

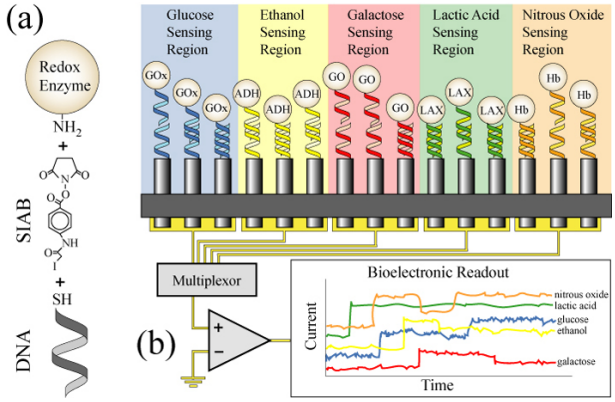

Figure 1. Site-addressable assembly of multiple enzymes to specific regions of a CNT array electrode. (a) The cross-linking of enzyme–ssDNA conjugates using the heterobifunctional cross-linker SIAB. An *N*-hydroxysuccinimide (NHS) ester reacts with an amine group on the enzyme while the iodoacetyl functional group reacts with a thiolated DNA oligo. (b) Parallel hybridization of the five enzymes used in this study to distinct regions of a CNT array electrode modified with differing ssDNA 'addresses' (not to scale). The CNTs are exposed from the aluminium oxide template on both sides. The top side is biofunctionalized while electrical contacts are made to the bottom side by gold evaporation. Electrocatalytic currents originating from the enzymes indicate the corresponding substrate concentrations.

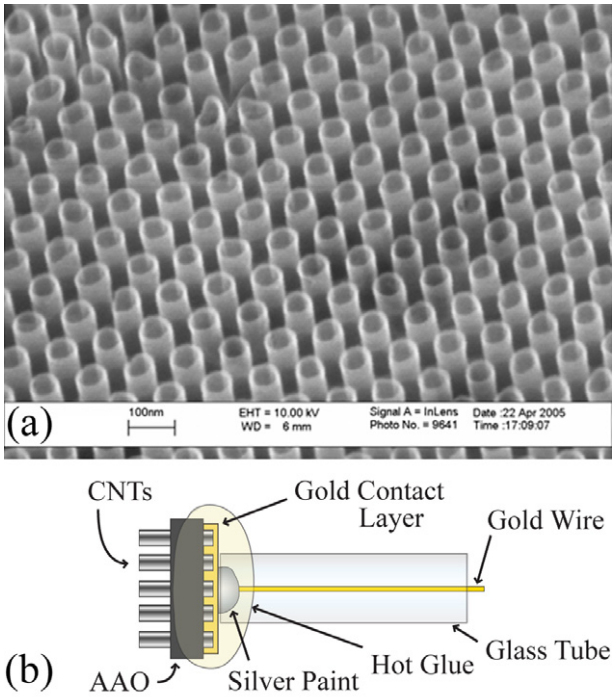

Figure 2. The highly ordered CNT array. (a) A scanning electron micrograph of the hexagonal array of aligned CNTs grown from an anodized aluminium oxide template (100 nm scale bar). (b) Construction of a single CNT array electrode.

sensors capable of monitoring multiple analyte concentrations at once [14]. With the continued scaling to systems of greater complexity, more sophisticated linking schemes that offer a greater degree of control over immobilization conditions will become necessary. It has been demonstrated that DNA can serve as a molecular link to address the site-specific delivery and binding of biomolecules and various surfaces [15–17]. In this study, we describe a DNA oligonucleotide linking scheme that enables the site-addressable delivery of a large number of different proteins to spatially distinct regions of a highly ordered CNT array, establishing an efficient electrical contact for direct electron transfer. The sequence specificity of DNA hybridization ensures that each enzyme carrying a single-stranded DNA (ssDNA) oligo tag will bind exclusively to the nanoelectrode region modified with the complementary single strand. This strategy is universally applicable to all proteins due to the simple conjugation chemistry involved. The heterobifunctional cross-linking agent *N*-succinimidyl[4-iodoacetyl]aminobenzoate (SIAB) is used to conjugate enzymes with thiolated ssDNA oligo tags (figure 1(a)) [18]. We have used this binding scheme to address the simultaneous assembly of five different redox-active enzymes: glucose oxidase (GOx), alcohol dehydrogenase (ADH), galactose oxidase (GO), lactate oxidase (LAX) and haemoglobin (Hb) onto our CNT array platform to form a multiplexed amperometric biosensor capable of monitoring levels of glucose, ethanol, galactose, lactic acid and nitrous oxide (NO) in real time (figure 1(b)). We have demonstrated the efficacy of the DNA-addressing scheme through the low occurrence of errant binding observed. By electrochemical methods, we have characterized each system and determined relatively high rates of electron transfer and substrate sensitivity. Further, we have performed studies to determine the degree of loss of enzymatic activity that occurs using this DNA-linking scheme, and the percentage of protein that is successfully electrically contacted to the CNTs. Finally, we have shown that metallization of the DNA link, which occurs at high pH levels in the presence of certain divalent metal cations [19, 20], significantly increases enzyme–nanoelectrode electron transfer efficiency. Overall, this DNA-linking strategy offers a relatively simple means of directing and controlling the nanoscale assembly of individual biomolecules and nanoelectronic elements while preserving high levels of biofunctionality and providing a stable physical link and an efficient electrical contact.

2. Experimental details

2.1. CNT fabrication and electrode construction

The electrodes used in this study were constructed using CNT array samples as the working electrode surface. The CNT array is fabricated by two-step anodization of high purity aluminium foil (∼99.999%, ESPI) followed by CNT growth by a chemical vapour deposition process. Further fabrication and post-fabrication processing details have been published previously by our group [21]. CNTs in this study are multi-walled CNTs measuring 20 nm in radius with a wall thickness of 2 nm and a 50 nm exposed length from the aluminium oxide nanopore template (figure 2(a)). To provide an electrical contact to the CNTs, a 100 nm gold layer was deposited onto the backside of the array using an e-beam evaporator (Thermionics Laboratory). A gold wire (0.127 mm, ESPI) was attached to this gold layer with silver paint (SPI Supplies), and

the wire was threaded through a glass tube (1.5 mm, Sutter Instruments). The contact interface between the array and the glass tube was sealed with hot glue (McMaster-Carr) to prevent exposure of the bare gold layer, gold wire or silver paint to the electrochemistry solutions (figure 2(b)). Active electrode surface areas were obtained by cyclic voltammetry (CV) in 0.5 M KNO_3 solution containing 0.02 M $K_3[Fe(CN)_6]$.

2.2. Bioconjugate preparation

All oligonucleotides used in this study were synthesized by Proligo (Sigma):

Name	Sequence	Modification
seqA	5′-GGTCCATTTCACACAGGA-3′	5′-amine
seqA′	3′-CCAGGTAAAGTGTGTCCG-5′	5′-thiol
seqB	5′-GTCAGCTGTGACCGTGAC-3′	5′-amine
seqB′	3′-CAGTCGACACTGGCACTG-5′	5′-thiol
seqC	5′-TGACGGAGATTGGGAGGC-3′	5′-amine
seqC′	3′-ACTGCCTCTAACCCTCCG-5′	5′-thiol
seqD	5′-AAGAAGCCCAGACGGAAA-3′	5′-amine
seqD′	3′-TTCTTCGGGTCTGCCTTT-5′	5′-thiol
seqE	5′-CTCGTCACCTAGCCAGGC-3′	5′-amine
seqE′	3′-GAGCAGTGGATCGGTCCG-5′	5′-thiol

Oligo sequences were adapted from those in the literature proven to exhibit high hybridization efficiency [22–24]. GOx from *Aspergillus niger*, ADH from *Saccharomyces cerevisiae*, GO from *Dactylium dendroides*, LAX from *Pediococcus sp.* and Hb from bovine blood were purchased from Sigma. The enzymes were dissolved in separate solutions of 50 mM, pH 8.3 sodium borate buffer (Sigma) and 5 mM EDTA (Sigma) to final protein concentrations of 0.1 mg ml^{-1} each. SIAB (Pierce) was dissolved in DMSO (Sigma) to make a 3.5 mM stock solution. 3 μl of SIAB stock was added to 1 ml of each protein solution, and the mixtures were allowed to react for 30 min at 25 °C. Two 1 ml Micro DispoDialyzers (Spectrum Laboratories) with a molecular weight cut-off (MWCO) of 3.5 kDa were conditioned using 50 mM sodium borate buffer, pH 8.3 for 30 min. The reaction mixtures were then transferred to the DispoDialyzer tubing to remove excess SIAB by dialysis at 4 °C for 12 h against a borate buffer solution, changing the 1 litre dialysis bath twice. The thiolated oligos seqA′, seqB′, seqC′, seqD′ and seqE′ were then added to the GOx, ADH, GO, LAX and Hb reaction mixtures, respectively, to a final concentration of 2 μM and allowed to react for 1 h at 25 °C in the dark. To cap any unreacted iodoacetyl groups on the SIAB cross-linker, cysteine (Pierce) was then added to the reaction mixtures to a final concentration of 5 mM and reacted for 15 min at 25 °C in the dark. Two 1 ml, 25 kDa MWCO Micro DispoDialyzers were conditioned to a 10 mM sodium phosphate buffer, 150 mM NaCl, pH 7.4 solution (PBS) (Sigma) for 30 min. Unreacted oligos and excess cysteine were removed by dialysis of the reaction mixtures in the DispoDialyzer and a 1 litre PBS dialysis bath at 4 °C, changed twice over 12 h. Enzyme–DNA conjugates were stored at 4 °C in PBS.

2.3. DNA addressing and hybridization

CNTs were functionalized with carboxylic acid groups by etching for 2 h in a 6 M H_2SO_4, 2 M HNO_3 solution (Sigma). The amine-terminated oligos seqA, seqB, seqC, seqD and seqE were covalently bound to the CNT array electrode to provide a distinct DNA 'address' to each sensing region. The covalent attachment was performed by first incubating the COOH-functionalized CNT array in 1-ethyl-3-(3-dimethylaminopropyl) carbodiimide hydrochloride (EDC; 200 mM, Biacore), NHS (50 mM, Biacore) and 2-(*N*-morpholino)ethanesulfonic acid (MES; 50 mM, Sigma) buffer for 1 h at 25 °C to form reactive esters from the carboxylic acid groups. The amine-terminated oligo was then added and incubated for 2 h at 25 °C to allow covalent binding. To prevent adsorption to the CNT side-walls, the CNT array was treated with GA (0.1% in PBS, pH 7.0, Aldrich), and subsequently washed with PBS to remove excess surfactant [25]. Hybridization of enzyme–DNA conjugates to the DNA-functionalized CNT array occurred in 100 mM NaCl, 50 mM phosphate buffer at pH 7.0, at an enzyme–DNA conjugate concentration of 0.1 mg ml^{-1}. The solution was heated to 40 °C and allowed to cool slowly to room temperature. Following hybridization, the CNT array was washed with hybridization buffer to remove unbound enzyme–DNA conjugates. For parallel addressing of multiple nanoelectrode regions, seqA–seqE were physically spotted onto separate, individually electrically contacted regions of the CNT array. The electrode was then immersed in a hybridization bath containing all conjugates GOx–seqA′, ADH–seqB′, GO–seqC′, LAX–seqD′ and Hb–seqE′. Hybridization conditions were applied as previously described (see above). Enzymes were assembled to their respective binding sites by sequence-specific hybridization. DNA metallization was carried out in 10 mM pH 9.0 Tris–HCl buffer (Sigma) containing 50 mM NaCl and 1 mM $ZnCl_2$ (Sigma).

2.4. Electrochemistry

All electrochemical measurements were recorded using a BAS potentiostat C3 cell stand with a three-electrode system consisting of the CNT array electrode as the working electrode, a platinum wire auxiliary electrode and a Ag/AgCl reference electrode. All trials were run in a 50 mM NaCl, 25 mM phosphate buffer saline (PBS) at pH 7.0 (Sigma) and 25 °C, unless otherwise noted. All solutions were deoxygenated by bubbling with argon for 20 min. All *CV* measurements were taken using a scan rate of 50 mV s^{-1}. During the multiplexed chronoamperometric (CA) measurements, redox potentials of +0.24 V, +0.18 V, +0.38 V, −0.12 V and −0.57 V were applied to the CNT electrode surfaces modified with GOx, ADH, GO, LAX and Hb, respectively, and the solution was stirred constantly using a magnetic stirrer (figure 3). Glucose, ethanol, galactose and lactic acid substrates were purchased from Sigma. NO gas was purchased from Corp Brothers. A saturated NO solution was prepared by first bubbling DIH_2O with argon for 30 min to remove O_2, which rapidly destroys NO. The solution was then bubbled through with NO gas for 30 min immediately before use and kept under an NO atmosphere at all times. The schedule of substrate

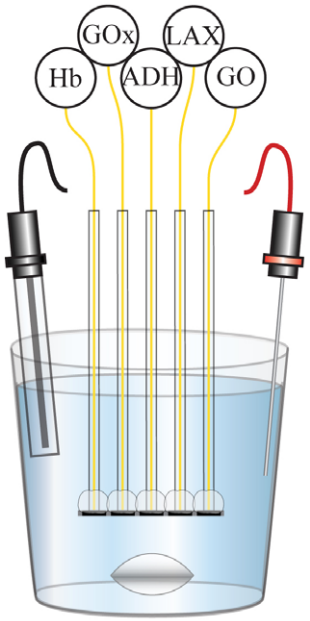

Figure 3. Experimental set-up for parallel detection of five substances. Ag/AgCl reference (black) and platinum counter electrodes (red) are used. The working electrode comprises five CNT array electrode regions with separate electrical contacts and distinct DNA 'addresses', each modified with a different redox enzyme as directed by sequence-specific hybridization of the DNA link. The regions (marked with labels) are contacted sequentially for CA measurement of each region, using an identical schedule of substrate injections for each measurement (see section 2.4). Alternatively, a multiplexor can be used for simultaneous measurement of all regions, as depicted in figure 1.

injections for CA measurement of each region is 1.5 mM NO, 20 mM glucose, 10 mM ethanol, 2 mM lactic acid and 20 mM galactose at 10, 20, 30, 40 and 50 s, respectively. For CA measurements of GOx in pH 9.0 10 mM Tris–HCl buffer to characterize the metallic DNA (M-DNA) link and corresponding controls, a redox potential of +0.17 V was applied.

2.5. Amplex® Red Assay

To quantify the total amount of active GOx bound to the CNT array, an Amplex® Red Glucose/Glucose Oxidase Assay Kit was purchased from Molecular Probes. The assay was performed on five different CNT array electrode samples according to the instructions provided with the kit. Fluorescent measurements were taken using a Quanta Master UV/vis fluorimeter (PTI). Experimental samples were compared to the calibration curve formed by standard solutions of 0, 0.1, 0.5, 1, 5 and 10 mU GOx.

2.6. Total GOx quantification by flavin adenine dinucleotide fluorescence

To quantify the total amount of bound GOx (active and inactive), the enzyme was first stripped from the CNT array by sonication for 2 h at 65 °C in deionized water (DIH_2O), which is sufficient for dehybridization of the short oligo duplex. Flavin adenine dinucleotide (FAD) extraction was then performed using a method previously described [26]. The enzyme was subjected to a 100 °C heat treatment for 5 min, followed by an addition of trichloroacetic acid (TCA, 5% w/v) for extraction of the flavin centre and precipitation of the protein. The protein was sedimented by centrifugation for 30 min at 14 000 rpm, leaving a clear yellow supernatant. The supernatant was removed and reserved, and the precipitate was washed with another volume of 5% w/v TCA for further flavin extraction. After a second centrifugation and supernatant extraction, the combined supernatant solution was neutralized with a 1 M K_2HPO_4 solution. Fluorescent measurements were taken using a Quanta Master UV/vis fluorimeter with an excitation wavelength of 465 nm and emission spectrum from 480–540 nm. Experimental samples were compared to the calibration curve formed by standard solutions of 0, 0.02, 0.05, 0.1, 0.2, 0.5 and 1 nM FAD (Sigma).

3. Results and discussion

There are two key system features that determine the overall function of bioelectronic devices: bioelectrocatalytic activity and the electrical contact between enzyme and electrode. Factors that influence system performance do so by affecting either or both of these features. Some such factors have been enumerated above: protein orientation, immobilization techniques and proximity to the electrode surface [5, 12]. Others include temperature, pH, ionic strength and the presence or absence of electron transfer mediators. These parameters, along with the attributes of the electrode platform itself, will dictate the level of enzymatic activity and the ability of the proteins to relay electrons to the electrode surface.

In order to evaluate our DNA-linking strategy in these terms, we performed three separate characterizations using GOx as a model enzyme to determine both the percentage of protein that remains active after hybridization to the array and also the percentage of the total active enzyme that is able to transfer electrons to the CNTs, from this point referred to as 'wiring efficiency'. First, the amount of active GOx that is electrically contacted to the array was determined by a well-established electrochemical method [27, 28]. *CV* measurements were taken in the absence of glucose before and after hybridization of GOx–seqA′ to a seqA-modified CNT array electrode (figure 4(a)). Since the substrate is not present, the reaction cannot turn over and each FAD centre that is contacted to the CNTs donates exactly two electrons (figure 4(b) (1)). By integrating the oxidation peak that arises after linking the enzyme to the electrode (shaded area, figure 4(a)), the total number of electrons transferred can be calculated and this value can be correlated to the number of successfully 'wired' GOx. Using this method, we found the surface enzyme coverage (SEC) of GOx made successful electrical contact to the CNTs $1.3 \pm 0.06 \times 10^{-12}$ mol cm^{-2}. It should be noted that the relatively large peak separation between oxidation and reduction peaks (∼0.18 V) suggests an irreversible process that arises from the overpotential needed to induce electron transfer across the DNA linker.

The second characterization quantified the total amount of active protein (both contacted and not contacted to the CNTs), using an Amplex® Red Glucose/Glucose Oxidase Assay Kit from Molecular Probes. In this assay, as glucose is converted to gluconic acid by GOx, H_2O_2 is formed as a by-product that in turn reacts with 10-acetyl-3,7-dihydroxyphenoxazine (the

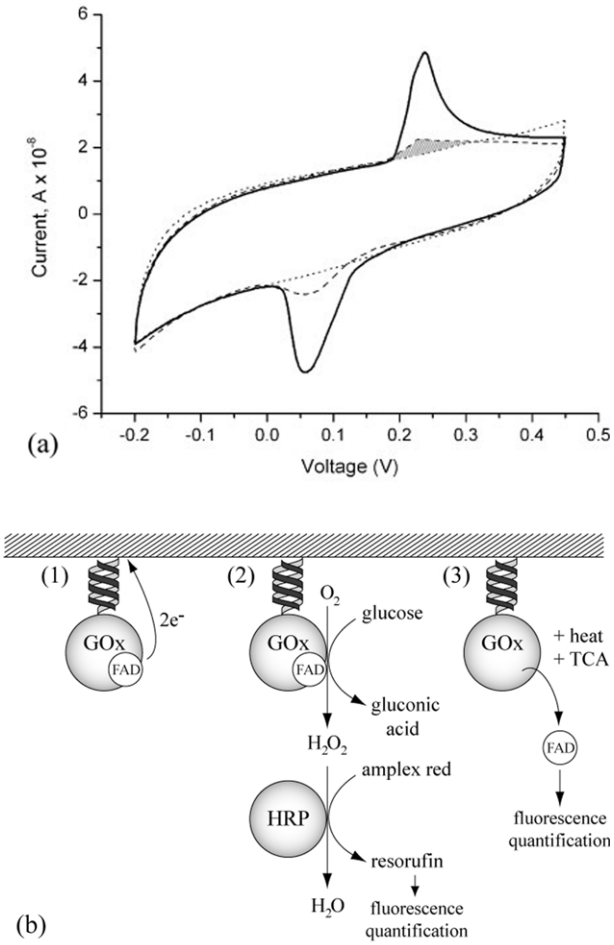

Figure 4. Quantification and characterization of GOx hybridized to the CNT array electrode via the DNA linker. (a) *CV* measurements taken in pH 7.0 PBS at 50 mV s^{-1} on a seqA-modified electrode (dotted curve), following hybridization of GOx–seqA′ conjugate to the array (dashed curve) and in the presence of 50 mM glucose (solid curve). The area of the oxidation peak in the absence of glucose (shaded area) is used to quantify the amount of GOx electrically contacted to the CNTs. (b) A schematic depiction of the three methods used to quantify the three states of GOx present. (1) CV measurement of GOx in the absence of glucose, resulting in the transfer of exactly two electrons from each FAD unit successfully contacted to the CNTs. This is a direct measurement of the quantity of GOx contacted to the CNTs. (2) Amplex® Red Assay in oxygenated buffer. As glucose is oxidized, molecular oxygen is reduced to H_2O_2. In the presence of HRP, H_2O_2 reacts with the amplex® Red Agent to form the red-fluorescent oxidation product resorufin. This product is quantified by fluorescence spectroscopy and compared to standard samples, indicating the total quantity of active GOx present. (3) The FAD redox centre is stripped from GOx using a heat treatment and 5% w/v TCA. FAD is then quantified by fluorescence spectroscopy and compared to standard samples, indicating the total quantity of GOx present (active and inactive).

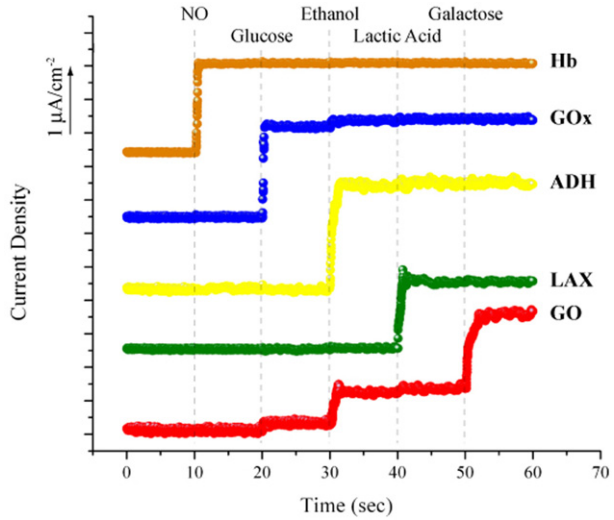

Figure 5. Parallel measurement of five different substrate concentrations in real time. CA measurements were performed on each separate CNT array electrode region in pH 7.0 PBS. A redox potential was applied corresponding to the enzyme for which each region is addressed. Substrates were injected in series at time intervals indicated by the dashed lines. Final concentrations after injections include: 1.5 mM NO, 20 mM glucose, 10 mM ethanol, 2 mM lactic acid and 20 mM galactose.

Amplex® Red reagent) in the presence of horseradish peroxidase (HRP) to generate the red-fluorescent oxidation product resorufin (figure 4(b), (2)). The rate of formation of resorufin is therefore directly related to the amount of active GOx present. It is a timed assay, with a fluorescent measurement taken after 30 min. Samples were compared against standard solutions, and the SEC of total active GOx was found to be $1.7 \pm 0.05 \times 10^{-12}$ mol cm^{-2}. Finally, to determine the total amount of GOx, both active and inactive, that is bound to the CNTs, we first removed all enzyme from the array by sonication for 2 h at 65 °C in DIH_2O, which is sufficient to dehybridize the short oligo duplex. We then extracted the flavin molecules from GOx using a heat treatment and 5% w/v TCA, followed by centrifugation of precipitated apoenzyme, leaving FAD in the supernatant (figure 4(b), (3)) [26]. FAD concentrations can readily be determined by fluorescence spectroscopy, and since each subunit of GOx contains a single FAD redox centre, the total amount of FAD present is equal to the amount of GOx bound to the array. After neutralization of the acidic solution with K_2HPO_4, fluorescent measurements were taken and compared against standard FAD solutions, indicating the presence of $1.9 \pm 0.06 \times 10^{-12}$ mol cm^{-2} of total GOx. By relating the total quantity of active enzyme to the total amount of GOx (active and inactive), we can conclude that $89 \pm 3\%$ of all protein that is physically linked to the CNT array by this DNA linking scheme retains its bioelectrocatalytic function. Furthermore, correlation of the active, contacted GOx to the total amount of enzyme reveals that $68 \pm 3\%$ of the total protein has established an efficient electrical contact to the CNTs. *CV* measurements taken in the presence of ethanol, galactose, lactic acid and nitrous oxide showed no peak current response (data not shown), indicating that the current response from the GOx-linked electrode is specific to glucose. Analogous measurements on ADH-, GO-, LAX- and Hb-linked electrodes showed similar specificities of these enzymes toward ethanol, galactose, lactic acid and nitrous oxide, respectively. The sole exception is GO, which is known to catalyse the oxidation of not only galactose but of all primary alcohols [31], and therefore shows some reactivity towards ethanol. The high degree of preservation

Table 1. Characterizations of five redox-active enzymes linked by DNA hybridization. (Note: Based on *CV* measurements in 25 mM PBS, pH 7.0 at a scan rate of 50 mV s^{-1}. For the five enzymes GOx, ADH, GO, LAX and Hb the substrates glucose, ethanol, galactose, lactic acid and nitrous oxide were used, respectively. Quoted uncertainties are based on measurements of five separate trials.)

Enzyme	Approx. linear response range ($\times 10^{-3}$ M)	Sensitivity ($\times 10^{-4}$ A M^{-1} cm^{-2})	Active SEC ($\times 10^{-12}$ mol cm^{-2})	Peak current density ($\times 10^{-6}$ A cm^{-2})	k_{ET} (s^{-1})
GOx	0–12	0.87	1.30 ± 0.1	1.72 ± 0.2	13.8 ± 1.4
ADH	0–50	1.0	4.96 ± 0.4	10.7 ± 0.8	22.4 ± 1.9
GO	0–10	0.77	1.92 ± 0.2	1.48 ± 0.1	8.0 ± 0.7
LAX	0–5	4.2	2.67 ± 0.3	2.90 ± 0.2	11.2 ± 1.0
Hb	0–2	8.9	3.78 ± 0.4	1.78 ± 0.1	4.9 ± 0.4

of enzymatic activity is probably due in part to the fact that the DNA linker acts as a molecular buffer between enzyme and electrode, establishing a single, non-denaturing point of contact. Covalent functionalization of CNTs is achieved by reacting with carboxylic acid groups that form in the presence of strong acids, primarily at the tips of the CNTs where they are most chemically active [29]. As such, this is the primary site of GOx attachment by DNA hybridization. Linking via CNT tips has been shown to preserve protein conformation and function due to the minimized point of contact and hydrophilic surface chemistry [6, 11].

In an analogous study, GOx attachment to a glassy carbon (GC) electrode surface via antigen–antibody binding revealed a comparable preservation of enzymatic activity [3]. In this approach, anti-rabbit IgG-labelled GOx was assembled onto an adsorbed rabbit IgG monolayer, showing virtually no loss in activity. Here again, the linker acts as a 'molecular cushion', shielding the enzyme from denaturing interaction with the electrode surface. This effect was highlighted when the activity of the antibody-linked GOx was compared to that of GOx directly covalently bound to the GC electrode surface. It was found that a 96% reduction in bioelectrocatalytic activity resulted from denaturing interaction with the flat, hydrophobic surface. Clearly, a linking agent that relieves this conformational stress can have a considerable impact on the performance of bioelectronic devices. The disadvantage of this antibody linking scheme is the sheer bulk of the linker which necessitates the inclusion of an electron transfer mediator in order to establish a conduction pathway to the electrode. Our DNA linker provides a sufficiently direct and non-obstructive contact so that direct electron transfer can occur.

Perhaps the standard for enzyme wiring is an approach demonstrated by Xiao *et al* [5], wherein apo-GOx was reconstituted onto AuNP-linked FAD, establishing a direct electrical contact between the enzyme and nanoparticle. The conjugate product was then linked to a gold electrode by a dithiol cross-linker and extremely high electron transfer kinetics was observed. Although clever and undeniably effective, it should be pointed out that stripping and reconstitution of enzymes and their redox centres are non-trivial, low-yield processes that require a high level of technical proficiency. Alternatively, our DNA wiring scheme involves simple, high-yield conjugation steps, making it better suited to more widespread use. Another benefit of the DNA interface when compared to adsorption and direct covalent attachment schemes is that its role as a semi-flexible linker may provide some degree of freedom for effective protein orientation [30]. An enzyme that is directly covalently attached to an electrode surface is fixed in place. The DNA linker provides a semi-flexible arm that can compensate for unfavourable orientation and potentially increase the number of binding orientations that can provide an effective electrical contact. Of course, the most significant qualitative advantage of the DNA linker is the addressability that DNA sequence-modulation provides.

This introduces true motivation for the incorporation of an addressable molecular linker such as DNA into bioelectronic designs, namely to provide a means of directing and controlling the self-assembly of biomolecules and nano-elements to allow for more sophisticated devices through greater multiplexing, increased lifespan and modular functionality. We have already demonstrated the use of the DNA linker to remove old enzyme after excessive loss of functionality over time by dehybridization of the link, followed by replacement with fresh protein for renewed functionality of the biosensor [14]. We have also reported the ability to use this same dehybridization/rehybridization method to swap different enzymes to adapt the biosensor to meet changing functional needs. In this study, we demonstrate the use of the DNA link to coordinate the simultaneous, parallel binding of the five different redox enzymes GOx, ADH, GO, LAX and Hb, each tagged with an ssDNA oligo of a different sequence (see section 2) to the different sensing regions of a CNT array platform modified with the complementary single strands. The resulting system constitutes a multiplexed biosensor capable of monitoring levels of glucose, ethanol, galactose, lactic acid and nitrous oxide in real time. To show the broad applicability of our enzyme–ssDNA cross-linking scheme using SIAB, we first performed an electrochemical characterization of each enzyme after hybridization to the CNT nanoelectrode to determine such key figures of merit as electron transfer rates (k_{ET} s) and substrate sensitivities (table 1). The calculation of k_{ET} s was performed as described previously [5, 6], correlating active SEC to peak current density. In the case of GOx, for example, we have measured a peak current density of 1.72×10^{-6} A cm^{-2} and an active, contacted SEC of 1.3×10^{-12} mol cm^{-2}.

By converting current density into terms of e^- s^{-1} cm^{-2}:

$$1.72 \times 10^{-6}\ \text{A cm}^{-2} = 1.72 \times 10^{-6}\ \text{C s}^{-1}\ \text{cm}^{-2}$$

$$(1.72 \times 10^{-6}\ \text{C s}^{-1}\ \text{cm}^{-2})/(1.6 \times 10^{-19}\ \text{C e}^{-1}) = 1.08 \times 10^{13}\ \text{e}^-\ \text{s}^{-1}\ \text{cm}^{-2}.$$

Dividing SEC by Avogadro's number:

$$(1.3 \times 10^{-12}\ \text{mol cm}^{-2}) \times (6.02 \times 10^{23}\ \text{GOx mol}^{-1}) = 7.83 \times 10^{11}\ \text{GOx cm}^{-2}.$$

And dividing the two values:

$$(1.08 \times 10^{13}\ \mathrm{e^-\ s^{-1}\ cm^{-2}})/(7.83 \times 10^{11}\ \mathrm{GOx\ cm^{-2}}) = 13.8\ \mathrm{e^-\ s^{-1}\ GOx^{-1}}.$$

We arrive at the electron transfer rate:

$$k_{\mathrm{ET}} = 13.8\ \mathrm{s^{-1}}.$$

k_{ET} is a direct measure of the number of electrons transferred per second from each enzyme to the electrode surface. The value of k_{ET} therefore provides information regarding the level of enzymatic activity and the efficiency of electron transfer at the enzyme–electrode interface. All enzymes in this study show efficient electron transfer kinetics and high levels of sensitivity over a broad dynamic range, indicating high levels of bioelectrocatalytic activity and efficient electrical contacts.

Five nanoelectrode regions with separate electrode contacts were each functionalized with a different ssDNA address (seqA–seqE). The five enzyme conjugates GOx–seqA′, ADH–seqB′, GO–seqC′, LAX–seqD′ and Hb–seqE′ were combined in a common hybridization bath and allowed to assemble to their respective CNT array regions directed by sequence-specific hybridization. The electrode was then placed into an electrochemical cell and CA measurements were taken with the corresponding redox potential applied to each CNT region. At 10 s intervals, each substrate was injected into the electrochemical cell in sequence, resulting in current steps from the various sensing regions (figure 5). Importantly, each sensing region responds only to the injection of the substrate of the enzyme for which it is addressed. The fidelity of electrocatalytic response of each region to injections of its proper substrate proves the efficacy of DNA addressability, as well as the specificity of each enzyme toward its respective substrate. The only significant exception is the CNT region functionalized with GO, which catalyses the oxidation of not only galactose but of all primary alcohols [31]. As such, the GO-functionalized region responds to both ethanol and galactose injections. In cases where the redox potential applied to a particular CNT region represents an overpotential for other enzymes used in the assay, it can be seen that a very small current step results from injections of the substrates of those enzymes. This response arises from trace amounts of randomly adsorbed protein. For instance, the CNT electrode region addressed for GOx binding (applied potential of +0.24 V) responds to the 20 mM glucose injection with a current density step of 1.35×10^{-6} A cm^{-2}, while the GO-addressed region (applied potential of +0.38 V) responds to the glucose injection with a 6.0×10^{-8} A cm^{-2} step in current density. As such, the magnitude of the response from randomly adsorbed GOx is only 4.4% that of the DNA-addressed response. Corresponding average adsorption response values for ADH and LAX are 5.2% and 4.1%, respectively. Therefore, in our system the average biosignal recorded from adsorbed protein is only 4.6% of that recorded from enzyme immobilized by sequence-specific DNA hybridization. This constitutes a low noise level that can easily be distinguished from the true signal.

It has been reported that native DNA can be converted to a novel form of DNA incorporating divalent metal cations under high-pH conditions (figure 6) [19, 20]. The mechanism of this conversion involves the displacement of an imino proton

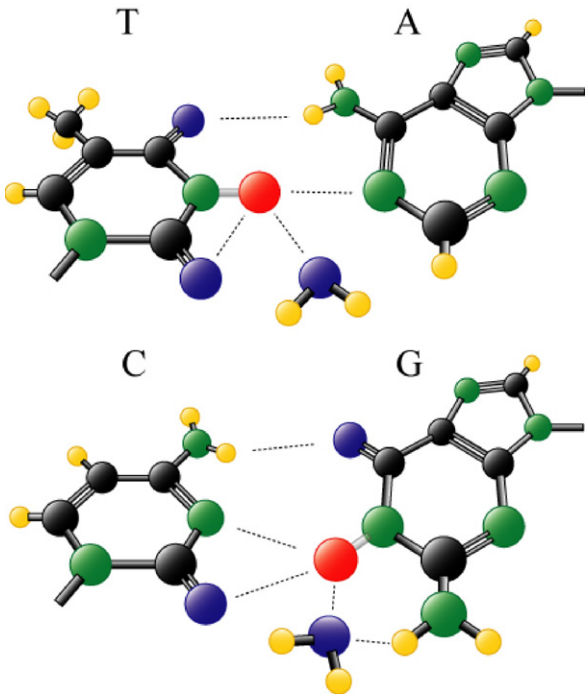

Figure 6. Proposed structure and base pairing scheme for M-DNA [19]. At high pH levels, the imino protons of the thymine and guanine base pairs are replaced by Zn^{2+}. Each base pair therefore coordinates a single Zn^{2+}, resulting in a continuous chain of divalent metal cations along the axis of the duplex. Hydrogen bonds are represented by dashed lines. Elements are represented as follows: hydrogen (), oxygen (), nitrogen (), carbon (), zinc ().

in the guanine and thymine base pairs by Co^{2+}, Ni^{2+} or Zn^{2+}. The resulting duplex, referred to as 'metallic DNA' (M-DNA), has been shown to exhibit metal-like conduction [20]. DNA conductivity is an issue of considerable controversy amongst bioelectronics scientists since it is difficult to distinguish conduction along the DNA strand itself from conduction through the high-ionic strength solution needed to preserve the structural integrity of the duplex [20, 32, 33]. For the purposes of our study, we do not intend to elucidate the actual mechanism of electron transfer along or around the DNA link, only to observe the result of metallization on increasing enzyme–CNT electron transfer. To try to distinguish the effect of metallization from that of simply increasing ionic strength by introducing metal cations, we have used Mg^{2+}, a non-M-DNA-forming metal cation [19] as a control. To characterize the metallized link, GOx was used again as the model enzyme, since it is fairly stable at high pH levels [34]. At the same time, native DNA was characterized at pH 9.0 for comparison, and DNA $+Mg^{2+}$ was studied as a control. In each case the active, contacted SEC was determined electrochemically as described above and correlated to the peak current density observed to calculate the k_{ET} s which are listed in table 2. It is evident that these rates are lower than that observed at pH 7.0. This is the result of decreased bioelectrocatalytic activity in high-pH solution. Regardless of this, there is a $64 \pm 5\%$ increase in k_{ET} via the M-DNA linker compared to native DNA. The Mg^{2+} control suggests that only $16 \pm 1\%$ of this increase in electron

Table 2. Characterization of the metallized DNA linker using GOx. (Note: Based on *CV* measurements in 10 mM, pH 9.0 tris-HCl buffer and 50 mM NaCl at a scan rate of 50 mV s^{-1}. Zn^{2+} and Mg^{2+} were added to final concentrations of 1 mM when used. 50 mM glucose was used as the substrate. Quoted uncertainties are based on measurements of five separate trials.)

Linker conditions	Active SEC ($\times 10^{-12}$ mol cm^{-2})	Peak current density ($\times 10^{-6}$ A cm^{-2})	k_{ET} (s^{-1})	Relative k_{ET} (%)
DNA	1.27 ± 0.1	0.69 ± 0.04	5.6 ± 0.4	100
DNA + Zn^{2+}	1.37 ± 0.1	1.21 ± 0.1	9.2 ± 0.7	164
DNA + Mg^{2+}	1.30 ± 0.1	0.82 ± 0.04	6.5 ± 0.4	116

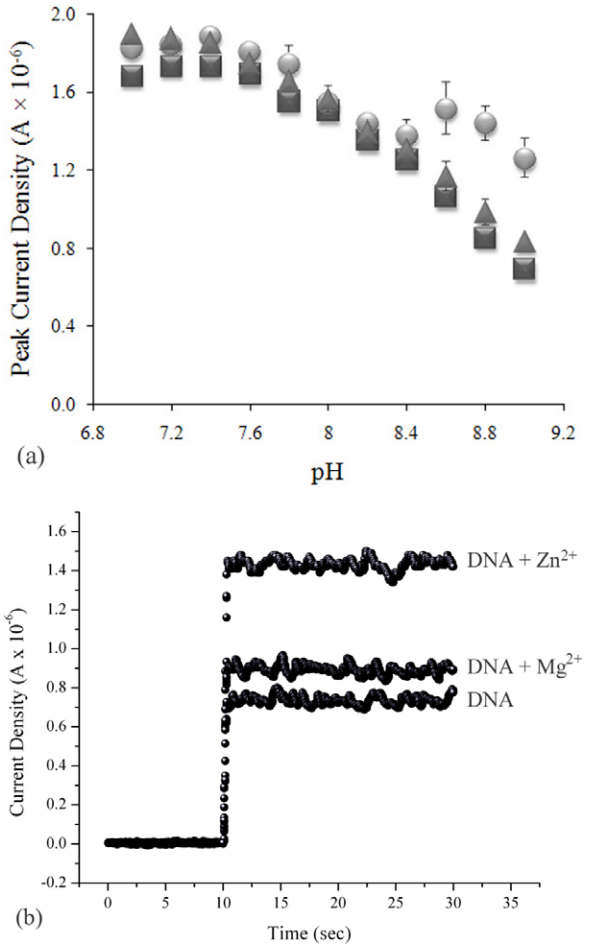

Figure 7. Evidence of increased electron transfer kinetics following metallization of the DNA link. (a) Peak current density taken from successive *CV* measurements in Tris–HCl buffer, 50 mM NaCl and 50 mM glucose as pH is increased from 7.0 to 9.0. There is a significant increase in peak current density in the presence of 1 mM $ZnCl_2$ above pH 8.6, the point of DNA metallization (●). No such increase is observed in the presence of non-M-DNA-forming $MgCl_2$ (▲) or the metal cation-free native DNA link (■). Error bars are not provided where the uncertainty is less than the size of the data point itself. (b) CA measurements taken in pH 9.0 Tris–HCl buffer and 50 mM NaCl, with an applied potential of +0.17 V. After 10 s, glucose is injected to a final concentration of 50 mM.

transfer efficiency is the result of the divalent metal cations in solution.

To further demonstrate the effects of metallization of the DNA link on enzyme–CNT electron relay, we measured the peak current density obtained through CV measurements in saturating glucose concentrations over a range of pH values (7.0–9.0), and plotted these current densities as a function of pH. Again, trials were performed in the case of DNA, DNA + Zn^{2+} and a DNA + Mg^{2+} control. As shown in figure 7(a), amid a decaying background that results from decreasing GOx activity in increasing pH, a pronounced increase in peak current is observed in the presence of 1 mM $ZnCl_2$ above pH 8.6, the established conditions required for M-DNA conversion [19, 20]. No such effect is seen in the case of the native DNA linker or in the presence of 1 mM $MgCl_2$, the divalent metal cation control. CA measurements were also taken for the three linker varieties at pH 9.0. A redox potential of +0.17 V was applied to the electrode. This negative shift from the redox potential of +0.24 V previously used for GOx results from the change in pH [35]. After 10 s, glucose was injected to a final concentration of 50 mM, resulting in current density steps from each of the three systems. These measurements are overlaid in figure 7(b). The relative magnitudes of the current density steps indicate increased linker conductivity in the case of the metallized DNA link.

4. Summary

We have introduced a novel DNA-linking strategy for the programmable assembly of highly multiplexed redox enzyme bio-nanoelectronic devices. The DNA linker is capable of site-addressable delivery of protein payloads to specific regions of a CNT array electrode platform modified with the complementary ssDNA tags. The linking process has been shown to preserve high levels of enzymatic activity and to establish an efficient enzyme–CNT electrical contact. We have demonstrated the assembly of five different enzymes to distinct nanoelectrode regions and used the conjugated system for the parallel monitoring of the concentrations of their corresponding five substrates in real time. Finally, we have metallized the DNA link by the addition of Zn^{2+} at high-pH conditions and observed elevated electron transfer kinetics when compared to the native DNA link. Because many enzymes show decreased bioelectrocatalytic activity under these metallization conditions, metallization may not be beneficial to all bioelectronic designs. However, the significant increase in linker conductivity observed suggests that it could be very effective in non-pH-sensitive systems as an addressable, self-assembling junction for nanoelectronic devices.

Acknowledgment

This work was made possible by generous support from the AFOSR through the MURI programme.

References

[1] Sung W J and Bae Y H 2006 *Sensors Actuators* B **114** 164
[2] Fan C, Li G, Zhu J and Zhu D 2000 *Anal. Chim. Acta* **423** 95
[3] Bourdillon C, Demaille C, Gueris J, Moiroux J and Saveant J M 1993 *J. Am. Chem. Soc.* **115** 12264
[4] Guiseppi-Elie A, Lei C and Baughman R H 2002 *Nanotechnology* **13** 559
[5] Xiao Y, Patolsky F, Katz E, Hainfeld J F and Willner I 2003 *Science* **299** 187
[6] Withey G D, Lazareck A D, Tzolov M B, Yin A, Aich P, Yeh J I and Xu J M 2006 *Biosens. Bioelectron.* **21** 1560
[7] Katz E, Buckmann A F and Willner I 2001 *J. Am. Chem. Soc.* **123** 10752
[8] Cai C and Chen J 2004 *Anal. Biochem.* **332** 75
[9] Zhao Y, Zhang W, Chen H and Luo Q 2002 *Anal. Sci.* **18** 939
[10] Yu X, Chattopadhyay D, Galeska I, Papadimitrakopoulos F and Rusling J F 2003 *Electrochem. Commun.* **5** 408
[11] Sotiropoulou S and Chainotakis N A 2003 *Anal. Bioanal. Chem.* **375** 103
[12] Katz E and Willner I 2004 *ChemPhysChem* **5** 1084
[13] Freire R S, Pessoa C A, Lucilene D M and Kubota L T 2003 *J. Braz. Chem. Soc.* **14** 230
[14] Withey G D, Kim J H and Xu J M 2007 *Nano and Giga Challenges in Electronics and Photonics Symp. (Phoenix, AZ)*
[15] Taft B R, Lazareck A D, Withey G D, Yin A, Xu J M and Kelley S O 2004 *J. Am. Chem. Soc.* **126** 12750
[16] Boozer C, Ladd J, Chen S, Yu Q, Homola J and Jiang S 2004 *Anal. Chem.* **76** 6967
[17] Li S, He P, Dong J, Guo Z and Dai L 2005 *J. Am. Chem. Soc.* **127** 14
[18] Chrisey L A, Lee G U and O'Ferrall C E 1996 *Nucleic Acids Res.* **24** 3031
[19] Aich P, Shaunivan L L, Tari L W, Delbaere L J T, Roesler W J, Falk K J, Steer R P and Lee J S 1999 *J. Mol. Biol.* **294** 477
[20] Rakitin A, Aich P, Papadopoulos C, Kobzar Y, Vedeneev A S, Lee J S and Xu J M 2001 *Phys. Rev. Lett.* **86** 3670
[21] Li J, Papadopoulos C and Xu J M 1999 *Appl. Phys. Lett.* **75** 367
[22] Niemeyer C M, Sano T, Smith C L and Cantor C R 1994 *Nucleic Acids Res.* **22** 5530
[23] Cattaruzza F, Cricenti A, Flamini A, Girasole M, Longo G, Prosperi T, Andreano G, Cellai L and Chirivino E 2006 *Nucleic Acids Res.* **34** e32
[24] Kohara Y, Noda H, Okano K and Kambara H 2002 *Nucleic Acids Res.* **30** e87
[25] Bandyopadhyaya R, Nativ-Roth E, Regev O and Yerushalmi-Rozen R 2002 *Nano Lett.* **2** 25
[26] Swoboda B E P and Massey V 1965 *J. Biol. Chem.* **240** 2209
[27] Willner I, Katz E, Patolsky F and Buckmann A F 1998 *J. Chem. Soc., Perkin Trans.* 2 **8** 1817
[28] D'Souza F, Rogers L M, O'Dell E S, Kochman A and Kutner W 2005 *Bioelectrochemistry* **66** 35
[29] Tsang S C, Chen Y K, Harris P J F and Green M L H 1994 *Nature* **372** 159
[30] Schuhmann W 2002 *Rev. Mol. Biotechnol.* **82** 425
[31] McPherson M J, Ogel Z B, Stevens C, Yadav K D S, Keen J N and Knowles P F 1992 *J. Biol. Chem.* **267** 8146
[32] Porath D, Bezryadin A, de Vries S and Dekker C 2000 *Nature* **403** 635
[33] Kasumov A Y, Kociak M, Gueron S, Reulet B, Volkov V T, Klinov D V and Bouchiat H 2001 *Science* **291** 280
[34] Zhu J *et al* 2002 *Sensors* **2** 127
[35] Liang W and Zhuobin Y 2003 *Sensors* **3** 544